BBA - Molecular Cell Research 1870 (2023) 119539

Contents lists available at ScienceDirect

BBA - Molecular Cell Research

journal homepage: www.elsevier.com/locate/bbamcr

Involvement of the alpha-subunit N-terminus in the mechanism of the Na^+, K^+-ATPase

B. Lev [a], M. Chennath [b], C.G. Cranfield [b], F. Cornelius [c], T.W. Allen [a], R.J. Clarke [d,e,*]

[a] School of Science, RMIT University, Melbourne, Vic, 3001, Australia
[b] School of Life Sciences, University of Technology Sydney, Ultimo, NSW 2007, Australia
[c] Department of Biomedicine, University of Aarhus, DK-8000 Aarhus, C, Denmark
[d] School of Chemistry, University of Sydney, Sydney, NSW 2006, Australia
[e] The University of Sydney Nano Institute, Sydney, NSW 2006, Australia

ARTICLE INFO

Keywords:
Salt bridge
Molecular dynamics
Replica exchange, zeta potential
Lipid-protein interaction
P-type ATPase
Gouy-Chapman theory

ABSTRACT

Previous studies have shown that cytoplasmic K^+ release and the associated E2 → E1 conformational change of the Na^+,K^+-ATPase is a major rate-determining step of the enzyme's ion pumping cycle and hence a prime site of acute regulatory intervention. From the ionic strength dependence of the enzyme's distribution between the E2 and E1 states, it has also been found that E2 is stabilized by an electrostatic attraction. Any disruption of this electrostatic attraction would, thus, have profound effects on the rate of ion pumping. The aim of this paper is to identify the location of this interaction. Using enhanced-sampling molecular dynamics simulations with a predicted N-terminal structure added to the X-ray crystal structure of the Na^+,K^+-ATPase, a previously postulated salt bridge between Lys32 and Glu233 (rat sequence numbering) of the enzyme's α-subunit can be excluded. The residues never approach closely enough to form a salt bridge. In contrast, strong interactions with anionic lipid head groups were seen. To investigate the possibility of a protein-lipid interaction experimentally, the surface charge density of Na^+,K^+-ATPase-containing membrane fragments was estimated from zeta potential measurements to be 0.019 (± 0.001) C m^{-2}. This is in good agreement with the charge density previously determined to be responsible for stabilization of the E2 state of 0.023 (± 0.009) C m^{-2} and the membrane charge density estimated here from published electron-microscopic images of 0.018C m^{-2}. The results are, therefore, consistent with an interaction of the Na^+,K^+-ATPase α-subunit N-terminus with negatively-charged lipid head groups of the neighbouring cytoplasmic membrane surface as the origin of the electrostatic interaction stabilising the E2 state.

1. Introduction

The P-type ATPase family of enzymes is a large group of integral membrane proteins found in all kingdoms of life which utilize the energy released by the hydrolysis of ATP to pump small ions, lipids and some other molecules across the membrane in which they are embedded. Two of the most widely studied are the ion pumps, the Na^+,K^+-ATPase and the H^+,K^+-ATPase, which are closely related and belong to the P2C group of the P2 subfamily of P-type ATPases. Both play crucial roles in animal cell physiology. The Na^+ electrochemical potential gradient created across the plasma membrane of animal cells by the Na^+,K^+-ATPase (or sodium pump) is used to drive nutrient reabsorption in kidney, and both the Na^+ and K^+ gradients it generates are essential for nerve and muscle function [1]. The H^+,K^+-ATPase (or proton pump) of gastric parietal cells creates the low pH of the stomach necessary for digestion [2].

Both proteins consist of a catalytic α-subunit and a much smaller β-subunit; in the case of the Na^+,K^+-ATPase there is a third even smaller subunit with a single membrane-spanning α-helix, which is termed the γ-subunit in kidney cells. A common feature of the α-subunits of both the Na^+,K^+- and H^+,K^+-ATPases is that they possess a lysine-rich N-terminal domain which extends into the cell cytoplasm [3] (see Fig. 1). If one defines the N-terminal domain as the protein sequence up to the start of the first transmembrane domain, then its length is around 75 residues for the Na^+,K^+-ATPase and 99 residues for the H^+,K^+-ATPase (both numbers based on the *Homo sapiens* proteins) [3]. The function of this domain, or even whether it has a function at all, is still an unsolved mystery in the field. In three-dimensional structures of the proteins

* Corresponding author at: School of Chemistry, University of Sydney, Sydney, NSW 2006, Australia.
E-mail address: ronald.clarke@sydney.edu.au (R.J. Clarke).

https://doi.org/10.1016/j.bbamcr.2023.119539
Received 11 May 2023; Received in revised form 26 June 2023; Accepted 10 July 2023
Available online 20 July 2023

determined by X-ray crystallography the complete N-terminal cytoplasmic domain could either not be resolved [4–7] or it was removed prior to crystal formation [8]. But the fact that its structure cannot be measured by X-ray crystallography doesn't necessarily mean that it doesn't play an important role, rather it simply implies that the N-terminal tail is either statically disordered, i.e., in different positions in different protein molecules within the protein crystal, or dynamically disordered, i.e., undergoing dynamic motion on the timescale necessary for X-ray data collection [9]. The N-termini of both proteins are predicted to be intrinsically disordered regions [3], with the degree of disorder in general increasing, as one would expect, as one proceeds from the first transmembrane helix to the start of the N-terminal tail. This would explain why the N-termini have not been resolved by X-ray crystallography.

A seemingly strong argument against the N-terminus playing an important role in the Na^+,K^+-ATPase was presented by Ohta et al. [10], who reported that the Na^+,K^+-ATPase of the frog *Rana catesbeiana*, also often referred to as *Lithobates catesbeiana* (American bullfrog), lacks the N-terminal lysine cluster, but still exhibits full Na^+,K^+-ATPase activity. This argument, however, has not stood the test of time. Ohta et al. [10] determined the amino acid sequence of the α-subunit by sequencing purified protein from the animal's kidney. In 2021 the protein was again sequenced from the same species but via nucleotide sequencing from the gene rather than from purified protein and it was shown that the animal's Na^+,K^+-ATPase does in fact possess a lysine cluster in its α-subunit N-terminal tail, as do all other animals investigated [11]. A possible explanation of Ohta et al.'s [10] result is that their protein may have undergone some degradation prior to sequencing. Thus, if the lysine cluster is present in all animals, it would seem likely that it does perform some important function.

The situation is the same in the H^+,K^+-ATPase. The authors are not aware of any animal species for which the α-subunit of the H^+,K^+-ATPase lacks a lysine-rich cytoplasmic N-terminus [3]. Asano et al. [12] carried out experiments with the H^+,K^+-ATPase expressed in HEK-293 cells, in which they replaced all of the positively charged lysine residues with uncharged alanine residues. They found that this had no effect on the stimulation of the enzyme's steady-state ATPase activity by ATP, K^+ or H^+. However, these results don't exclude a role of the N-terminus in determining ion pump kinetics, because there remains the possibility that the N-terminus could play a role in the conformational change of the unphosphorylated enzyme, E2 → E1, which is necessary for K^+ deocclusion and release into the cytoplasm. That the N-terminus could affect this transition would seem reasonable, considering its location on the cytoplasmic face of the protein. Unfortunately very little information is currently known about the kinetics of this reaction for the H^+,K^+-ATPase. Some kinetic data were recently presented by Faraj et al. [13], which showed that the E2 → E1 occurred in the second-subsecond timescale. However, their studies were carried out using the fluorescent probe eosin, which is known to bind to the cytoplasmic nucleotide binding site of the protein [14], and this could influence the rate of the transition.

Much more extensive data is available on the Na^+,K^+-ATPase and the role of its N-terminus. The first indications of an important role of the lysine-rich N-terminus in the E2 → E1 transition and associated K^+ release to the cytoplasm came from trypsin digestion experiments carried out by Jørgensen and co-workers [15–18], who showed clear differences in the cleavage of the N-terminus in the E2 and E1 states, thus indicating significant movement of the N-terminus during the transition. Specifically, they found that Lys^{30} of the N-terminus is in an environment where it is much more protected from trypsin attack in the E2 state than the E1 state. Furthermore, because it was found that trypsinolysis of the bond 30–31 was strongly dependent on ionic strength [16,18], Jørgensen and Collins [15] suggested that a salt bridge is involved in the E1 → E2 transition. From stopped-flow kinetic investigations utilizing the probe RH421 as well as measurements of conformational distribution using eosin [19], we have provided strong support for this suggestion, with an electrostatic attraction stabilising the E2 state and breaking of the interaction allowing the enzyme to convert to the E1 state. Further strong supporting evidence for the involvement of the N-terminus in the E2 → E1 transition has been found by the group of Blostein, who found [20] that removal of the N-terminus accelerated the rate of K^+-deocclusion of enzyme purified from dog kidney. In subsequent experiments in which they expressed rat Na^+,K^+-ATPase in HeLa cells and investigated the effect of various mutations [21,22], they confirmed their results on purified enzyme and localized the cause of the effect of the N-terminus on K^+ deocclusion to residues 24–32, i.e., ERDMDELLK, which include the site of trypsin cleavage. Cornelius et al. [23] showed that the effect of the N-terminal truncation in shifting the E1-E2 conformational equilibrium towards E1 was not restricted to mammalian enzymes, but also occurred in shark Na^+,K^+-ATPase. Wu et al. [24] investigated via electrophysiological experiments the role of the N-terminus of electric ray, *Torpedo californica*, Na^+,K^+-ATPase expressed in *Xenopus laevis* oocytes, increasing the measurable currents significantly by converting the Na^+,K^+-ATPase into a channel via the selective-binding molecule palytoxin. Their results led them to conclude that the N-terminus acts as an inactivation gate on the cytoplasmic side of the protein, preventing K^+ release, in an analogous fashion to the N-terminus of *Shaker* K^+ channels. Earlier electrophysiological measurements by Burgener-Kairuz et al. [25] had shown an effect of N-terminal truncation on K^+-induced activation of Na^+,K^+-ATPase pump currents in *Xenopus* oocytes on the protein's extracellular face, but they didn't investigate the cytoplasmic face where the N-terminus is located and hence where one would expect more dramatic effects from truncation. Very recently, structures of the Na^+K^+-ATPase were determined by Nguyen et al. [26] and Guo et al. [27] via cryoelectronmicroscopy which provided more information of the enzyme's cytoplasmic ion gating mechanism. Although the N-terminus still couldn't be resolved, these structures showed that cytoplasmic gating involves significant movement of the protein's first transmembrane helix. Because the N-terminus is directly covalently linked to the first transmembrane helix, this supports the idea that cytoplasmic gating involves significant movement of the N-terminus, as previously suggested by Jørgensen and coworkers based on biochemical data alone [15–18].

Experimental evidence also exists, however, which argues against an

Na^+,K^+-ATPase

GVGRDKYEPAAVSEQGDKKGKKGKKDRDMDELKKEVSMDDHKLSLDELHRKYGTDLSRGLTSARAAEIL
ARDGPNA...

H^+,K^+-ATPase

GKAENYELYSVELGPGPGGDMAAKMSKKKKAGGGGGKRKEKLENMKKEMEINDHQLSVAELEQKYQT
SATKGLSASLAAELLLRDGPNALRPPRGTP...

Fig. 1. N-terminal sequences of the *Homo sapiens* Na^+,K^+-ATPase and H^+,K^+-ATPase α_1-subunits. The basic amino acid residues, lysine (K) and arginine (R), are highlighted in blue. The acidic amino acid residues, aspartic acid (D) and glutamic acid (E), are highlighted in red. Ignoring any partial protonation of histidine residues (H) and any local environmental effects on sidechain pKa values, the total charges of the N-terminal sequences shown would be expected to be +3 for the Na^+,K^+-ATPase and + 4 for the H^+,K^+-ATPase. (For interpretation of the references to colour in this figure legend, the reader is referred to the web version of this article.)

important role of the N-terminus in Na^+,K^+-ATPase function. Shanbaky and Pressley found [28] that after expression of a mutant Na^+,K^+-ATPase with an altered N-terminus in a COS-1 cell line, the cells maintained their viability and they observed no significant changes in Na^+, K^+-ATPase enzymatic activity. They did not, however, investigate K^+ deocclusion, which, as described above, is the reaction others have found to be most affected by removal of the N-terminus. Furthermore, one must be careful is extrapolating results found with cultures of cell lines to natural cells, particularly when dealing with membrane proteins. It has been found that the fatty acid profile of the membranes of cultured cells varies significantly from that of natural cells [29]. In addition, cancer cells, on which many cell lines are based, display an exposure of phosphatidylserine on the extracellular surface of the plasma membrane [30–32], whereas under most conditions flippase activity in noncancerous cells ensures that phosphatidylserine is located almost exclusively in the cytoplasmic leaflet of the plasma membrane [33]. Therefore, if the interaction of the N-terminus which stabilises the E2 state relative to the E1 state is with anionic phospholipids, such as phosphatidylserine, as some studies have suggested [19,33–36], it is likely that very different results could be observed between cultured and native cells. The group of Blostein [37–39], however, have identified another possible interaction partner of the N-terminus, namely Glu233 (numbering excluding the propeptide sequence MGKGV) in the first M2-M3 cytoplasmic loop of the α1-subunit. The aim of this paper is to consider the likelihood of these possibilities by means of determining the charge density of Na^+,K^+-ATPase-containing membrane fragments and by the use of enhanced-sampling all-atom molecular dynamics (MD) simulations.

2. Materials and methods

2.1. Enzyme and reagents

Na^+,K^+-ATPase-containing membrane fragments from pig kidney outer medulla were purified as described by Klodos et al. [40]. The specific ATPase activity at 37 °C and pH 7.0 was measured according to Ottolenghi [41]. The activity of the preparation used was 1400 μmol ATP hydrolysed h^{-1} (mg of protein)$^{-1}$ at saturating substrate concentrations in a buffer containing 20 mM histidine, 250 mM sucrose and 0.9 mM EDTA. The protein concentration was 4 mg mL^{-1}, determined by the Peterson modification [42] of the Lowry method [43] using bovine serum albumin as a standard.

The reagents used for buffer preparation were; sucrose (≥99.5 %, Sigma-Aldrich, Castle Hill, Australia), L-histidine (≥99.5 %, Sigma-Aldrich), EDTA (99 %, Ajax Finechem, Scoresby, Australia), imidazole (≥99 %, Sigma-Aldrich), and NaCl (≥99.5 %, Panreac Applichem, Barcelona, Spain).

2.2. Zeta potential measurements

The zeta potentials of Na^+,K^+-containing membrane fragments diluted into buffer solutions of varying ionic strength were determined using a Nano-ZS Zetasizer (Malvern Instruments, Malvern, UK). Measurements were performed within DTS1070 folded capillary cells (ATA Scientific, Taren Point, NSW, Australia). The Nano-ZS Zetasizer measures the zeta potential of a colloidal particle via the technique of phase analysis light scattering using the 632.8 nm line of a 4 mW He—Ne laser and a scattering angle of 173°. In brief, the technique measures the zeta potential from the difference in phase of scattered versus non-scattered light arising because of the electrophoretic velocity of the colloidal particles, which depends on the magnitude of their surface charge density [44].

To avoid interference from scattering due to dust particles, the buffer solutions used for dilution of the Na^+,K^+-ATPase-containing membrane fragments were first filtered through 0.22 μm pore-size hydrophilic Teflon syringe filters (Nantong FilterBio Membrane, Jiangsu, China). The final concentration of Na^+,K^+-ATPase used within the capillary cell was 0.62 mg/ml. All zeta potential values reported are the average of six measurements.

2.3. Molecular dynamics simulations

To investigate the behaviour of the Na^+,K^+-ATPase with a reconstructed N-terminal sequence and its interactions with lipid bilayers in the presence of 1,2-dioleoyl-sn-glycero-3-phospho-L-serine (DOPS), 1,2-dioleoyl-sn-glycero-3-phosphocholine (DOPC), and cholesterol, we have carried out molecular dynamics (MD) simulations. Available structures for pig kidney Na^+,K^+-ATPase in an E1P-like state (PDB 3WGU [6]) and the E2 state (PDB 3B8E [4]) with the secondary structure of first 40 N-terminal residues reconstructed (using the Galaxy method in CHARMM-GUI [45]), were embedded in bilayers containing 26 mol% DOPC, 34 mol% DOPS and 40 mol% cholesterol. These compositions were chosen based on the native lipid composition of the membranes from which the enzyme originated, as determined by biochemical analyses [46,47], but with an anionic lipid content with an absolute magnitude 12 % higher and, on a relative basis, 52 % higher than what one would expect physiologically from the biochemical data and the expectation that PS would be concentrated in the cytoplasmic leaflet due to flippase activity, i.e., more physiological values would be 38 mol% PC, 22 mol% PS and 40 mol% cholesterol. The protein constructs were immersed in 150 mM NaCl solution using explicit TIP3P water molecules. The lipid distribution within the membrane was randomised with CHARMM-GUI [45].

The systems were then equilibrated using NAMD 2.9 [48] with the CHARMM36 force field [49,50]. The temperature was maintained at 303.15 K using a Langevin thermostat and pressure maintained at 1 atm using the Nose-Hoover Langevin piston method [51] with rectangular periodic boundary conditions. All bonds to hydrogen atoms were maintained using the SHAKE algorithm [52]. Electrostatic interactions were computed using the Particle Mesh Ewald method [53] with a grid spacing of 1 Å. Non-bonded pair lists were recorded to 16 Å with a real space cut-off of 12 Å using energy switching from 10 Å. Each system was run for 700–900 ns to fully relax the protein in the membrane environment and explore N-terminal interactions with the surrounding protein and membrane. Two independent simulations were run for starting structure 3WGU and two for 3B8E in the aforementioned bilayers containing PS lipids. A further two independent simulations for each model were carried out without PS lipids, totalling 6.4 μs of MD simulation. One such MD simulation system, based on the E2 state of the Na^+,K^+-ATPase α_1 subunit (PDB 3B8E) with the N-terminus added, following MD simulation, is shown in Fig. 2.

Analysis of these 8 independent MD simulations for each structure and each bilayer revealed little dynamics, with the N-terminus largely remaining either in contact or away from the membrane, with no reproducibility between the independent copies of the simulation (see Fig. S1). We judged from this that regular free MD simulation, even on this large scale, are incapable of properly sampling the N-terminal interactions. We instead turned to Replica Exchange Solute Tempering (REST2) simulations [54]. This method requires simulation of several copies of the system (16 systems for 0.2 μs each), with N-terminal interactions systematically weakened (with higher effective temperatures of 300-600 K) to speed up movements exponentially, exchanged via regular Monte Carlo moves. The first 40 residues were chosen for scaling, with exchanges attempted every 100 fs over the duration of each 200 ns simulation. Separate REST2 simulations were carried out for 3WGU and 3B8E models, following the unbiased MD, totalling a further 6.4 μs of MD simulation. This approach resulted in good sampling of N-terminal dynamics and interactions with protein and lipids, as illustrated in the sample Supporting Movies 1-6; with good exchange between the 16 replicas over the simulations (Fig. S2).

Analysis presented in Fig. 3 is for the physical/base replica 0 (effective temperature 300 K for N-terminal interactions), but the full range of replicas has been studied and reported, in part, in the Supporting

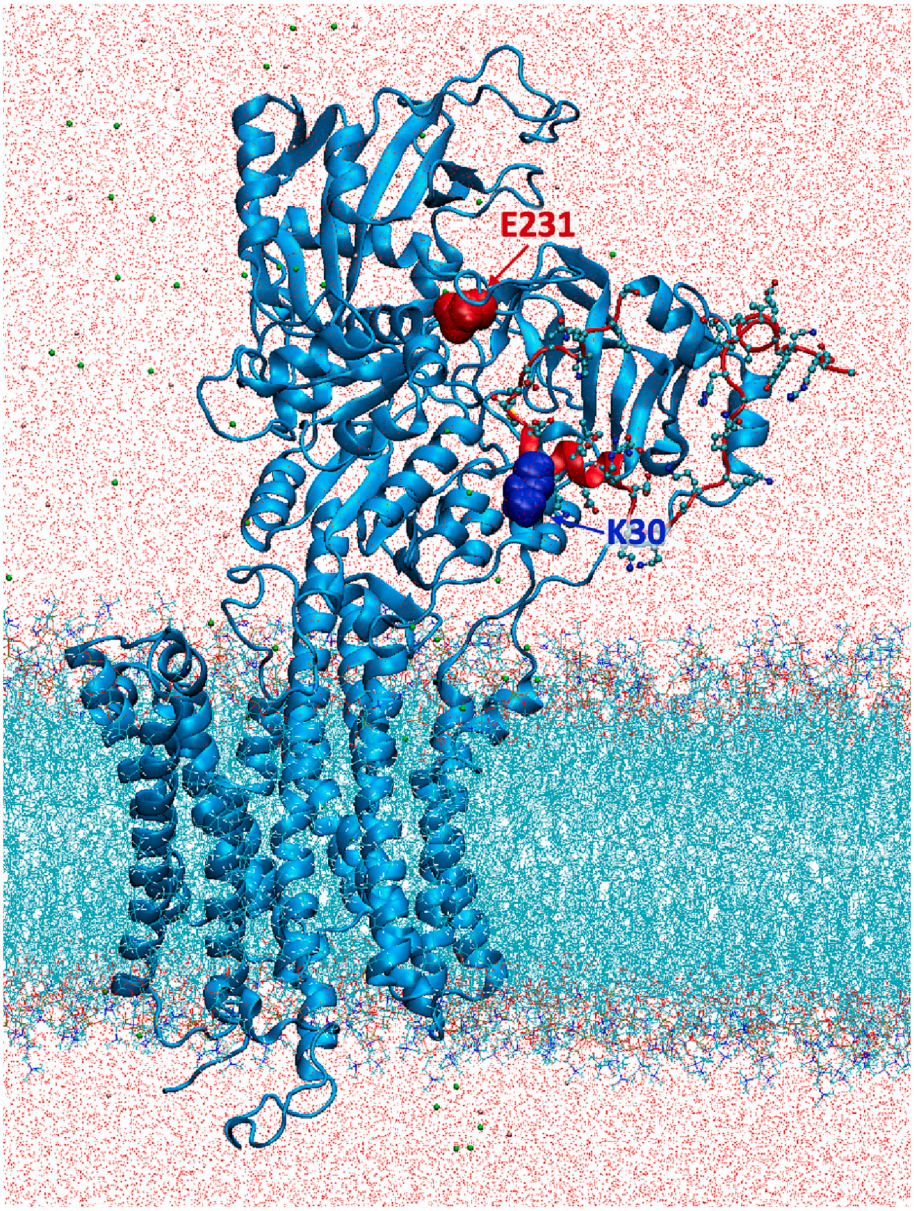

Fig. 2. MD simulation system. Shown is one sample MD simulation system based on the structure of the E2 state of the α_1 subunit of pig Na^+,K^+-ATPase (using PDB 3B8E [4] with the N-terminus added). The protein is shown as blue ribbon, with the N-terminus (first 40 residues) highlighted in red with side chains as ball-and-stick representation. Lipids are shown with cyan stick for tails and CPK-coloured head-groups, with water molecules as red dots (Na^+ and Cl^- ions as small pink and green balls). The configuration shown is following unbiased MD simulation to relax the protein in the membrane. Highlighted in red and blue are residues E231 and K30, respectively. (For interpretation of the references to colour in this figure legend, the reader is referred to the web version of this article.)

Figs. 2–4. Interaction between the proposed Lys30 and Glu231 (pig Na^+, K^+-ATPase α_1-isoform numbering) in Fig. 3a and Fig. S3 is based on calculations of probabilitiy distributions for the distance between the lysine ammonium N atom (as opposed to the individual H atoms) and the glutamate carboxylate's central C atom (as opposed to the individual atoms), with salt bridge considered to have formed if the distance is less then 4.5 Å (based on a Lys N - Glu C radial distribution function; not shown). Analysis of interactions between basic residues of the N-terminus and lipid head groups (as shown in Fig. 3b and Fig. S4) involved the calculation of probability distributions (unnormalised, as distinct from a radial distribution function) between any R or K side chain N atom and any lipid head group (PS or PC) O atom. The cut-off for a direct coordinating contact (i.e., the formation of a salt bridge between the positively charged R or K and the negatively charged head group moiety) was chosen to be 3 Å (based on a radial distribution function for N—O distance; not shown). This analysis was decomposed into individual basic residues of the N-terminus in Fig. S3. Errors in contact probabilities are reported as ± one standard error of means based on 6 blocks of data. The analysis was carried out separately for interactions between the N-terminus with PS or PC lipid headgroups.

3. Results

3.1. Investigation of possible interaction between Lys32 and Glu233 and between the N-terminus and the surrounding membrane

The Blostein group [37–39] have suggested a possible regulation of the Na^+,K^+-ATPase via an interaction of the N-terminus, specifically Lys32 (corresponding to Lys30 in the pig Na^+,K^+-ATPase α_1-isoform) via a salt bridge with Glu233 of the rat α_1-isoform (corresponding to Glu231 in the pig Na^+,K^+-ATPase α_1-isoform). They made this suggestion based on mutagenesis studies before a crystal structure of the Na^+,K^+-ATPase was available. If they formed deletion mutants lacking either the first 16 or the first 23 amino acid residues of the N-terminus, they found [55] that the Na-ATPase activity of the mutants resembled the wild-type enzyme. However, if they deleted the first 32 amino acid residues, the mutant enzyme showed a much-reduced inhibition by K^+ ions relative to the native enzyme, suggesting a role of the N-terminus in the K^+-deocclusion reaction on the cytoplasmic face of the protein. The fact that this change in enzyme behaviour occurred on increasing the number of deleted residues from 23 to 32 indicates that the nine residues Glu24-

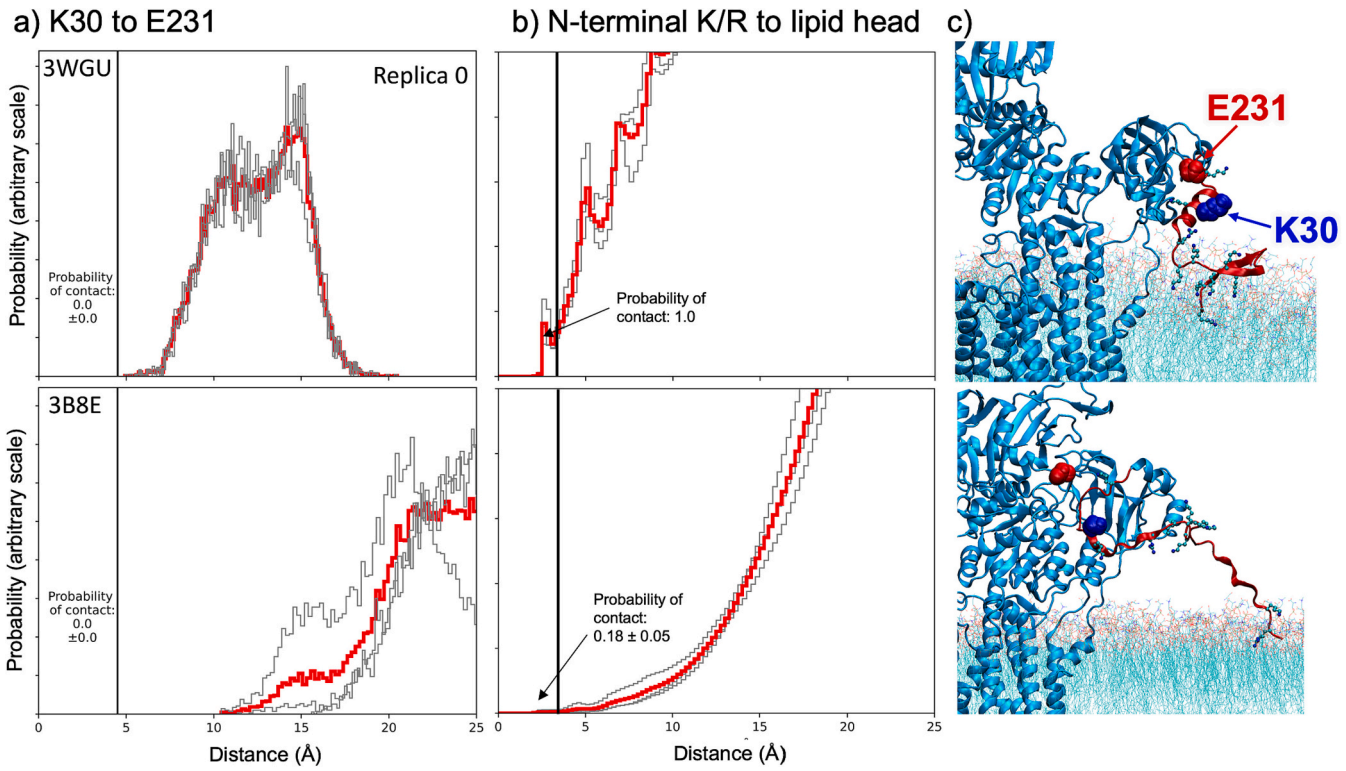

Fig. 3. N-terminal interactions. (a) Histograms of probabilities for the distance of separation between Lys30 and Glu231 (pig sequence numbering) from REST2 simulations. The replica 0 simulations shown represent a temperature of 300 K (i.e., 27 °C; see Fig. S3 for other replicas). The grey lines correspond to 3 blocks of data from the same simulation (200 ns per replica split into 3 chunks) to reveal the extent of variation. The red curves represent the complete distribution determined with all 200 ns MD. The upper panel, calculated using PDB file 3WGU, shows the expected distribution of distances in a Na^+-bound conformation preceding the E1P state [6]. The lower panel, calculated using PDB file 3B8E, shows the corresponding distribution for the E2 state [4]. The radius for the black line is 4.5 Å, representing a cut-off for salt-bridge formation based on a Lys N and Glu carboxylate C radial distribution function. In both states the probability of salt bridge formation between K30 and E231 is zero (although it is seen in replicas with elevated temperatures to a small degree; see Fig. S3). (b) Histograms showing the probability distribution (unnormalised) for the interaction between any N-terminal K or R side chain N—H group and any lipid head group O atom. The radius for the black line is 3 Å, representing a cut-off for salt-bridge formation based on a radial distribution function for N—O distance. For 3WGU, the probability of forming a salt bridge is 100 % in this base replica, but this interaction is gradually lost in elevated replicas (see Fig. S4a), indicative of good sampling (see also Supporting Movies 1–3; revealing a dynamic N terminus). For 3B8E, the probability of direct contact/salt-bridge formation with lipids is 18 ± 5 %, still being significant, but with the N-terminus residing mostly away from the membrane (see Fig. S4b and Supporting Movies 3–6). Histograms have been plotted with different normalisations (arbitrary scales) to best illustrate their distributions (panel a normalised to ensure a total of all distances for the pair of atoms summing to 1; panel b unnormalised, with a different scale due to the many different atom pair distances involved). (c) The right column shows sample snapshots illustrating lipid interactions in each structure, although this is best captured in the Supporting Movies. (For interpretation of the references to colour in this figure legend, the reader is referred to the web version of this article.)

Arg-Asp-Met-Asp-Glu-Leu-Lys-Lys32 (rat sequence) must play an important role in determining the enzyme's response to K^+. In the pig, the sequence is identical, but the numbering is residues 22–30, because the pig α_1 subunit is missing residues 17 (lysine) and 18 (serine) of the rat sequence.

Now that crystal structures have been solved in different conformational states [4–7], it has become possible to investigate the plausibility of a Lys32-Glu233 salt bridge from a structural perspective (see Fig. 2 for the locations of these residues). Based on X-ray crystallographic studies of the model compound ammonium formate [55], to form a salt bridge a hydrogen atom attached to the side chain ammonium group of Lys32 and an oxygen atom of the side chain carboxylate group of Glu233 would have to be located within 2.81–2.89 Å of one another. Based on analysis of the neighbouring lysine N and glutamate C_z radial distribution function, this corresponds to a distance cut-off of ~4.5 Å. REST2 simulations using the structure of pig kidney Na^+,K^+-ATPase in the E1P state (3WGU) and E2 state (3B8E) [4] show no salt bridge formation between these residues in the physical/base replica (see Fig. 2a). This was true for all replicas of the 3B8E REST2 simulation (see Fig. S3b). For 3WGU we also observed no K-E contact in the low-lying replicas, with only the highly elevated (unphysical) replicas showing non-negligible K-E contact (see Fig. S3a). Based on these simulations, a direct interaction between Lys32 and Glu233 can be excluded.

This does not necessarily mean that Glu233 plays no important role in the Na^+,K^+-ATPase mechanism, including K^+ deocclusion. Indeed, alignment of vertebrate α_1-subunit sequences of the Na^+,K^+-ATPase show that Glu233 is a conserved residue. Therefore, it very likely does play some important mechanistic role, but this does not appear to be via a direct interaction with Lys32.

If the N-terminus isn't interacting with Glu233, then where does it interact? Fig. 3b and c (upper panels) show analysis of the base replica for the E1P (3WGU) and E2 (3B8E) state simulations for the distribution of distances between the basic side chains of the N-terminus and the lipid head groups. This analysis reveals that the N-terminus in the E1P simulations has very strong and sustained interactions with PS head groups throughout the simulation (see also Supporting Movie 1). In replicas with elevated effective temperatures (Fig. S4a and Supporting Movies 2 and 3), the interaction gradually weakens (being very dynamic for intermediate replicas and lost in high temperature replicas), but it is clearly a strong determinant of the N-terminal structure.

For the E2 (3B8E) simulation, Fig. 3b and c (lower panels) reveal direct contact with lipid headgroups on and off during the simulations, where 18 ± 5 % of the time the N-terminal basic residues were forming

salt bridges with the lipid head groups (see also Supporting Movie 4). Higher replicas (Fig. S4b) showed a gradual reduction in lipid contacts as N-terminal interactions were scaled back, as expected. For intermediate replicas (e.g. replica 4; Supporting Movie 5), the dynamic N-terminus was seen to bind and dissociate from the membrane over the simulation, eventually completely dissociating for high temperature replicas (Supporting Movie 6).

For the simulations of both the E1P and E2 states the results show that almost all N-terminal salt bridge formation is with charged PS head groups. The calculated overall probabilities for PC and PS binding to N-terminal residues for 3B8E of 0.004 ± 0.003 and 0.17 ± 0.05, respectively, and for 3WGU they are 0.018 ± 0.006 and 0.9992 ± 0.0004. This says that, on average, N-terminal residues contact PS head groups 51 ± 4 times more often than the zwitterionic PC head groups.

3.2. Zeta potential measurements

Previously we have successfully used Na^+,K^+-ATPase-containing membrane fragments to study the role of an electrostatic interaction that stabilises the E2 conformation and whose breakage leads to the transition into the E1 conformation [19]. At that time, we proposed that the electrostatic interaction could be between the N-terminus and the surrounding membrane surface. Here we test this hypothesis by measuring the zeta potential, ψ_z, of the membrane fragments, from which we derive the surface charge density, σ, of the membrane. According to the Gouy-Chapman theory [56,57], the decay of the electrical potential, ψ, in the solution adjacent to a charged surface can be approximated by an exponential relation as the distance, r, from the surface increases. Thus,

$$\psi = \psi_0 exp(-r/l_D) \tag{1}$$

where ψ_0 is the electrical potential at the surface and l_D is the Debye length, which is defined by the following expressions:

$$l_D = \frac{1}{F}\sqrt{\frac{\varepsilon_0 \varepsilon RT}{2I}}, \tag{2}$$

$$I = \frac{1}{2}\sum_{i=1}^{n} c_i z_i^2 \tag{3}$$

F is here Faraday's constant, ε_0 is the electrical permittivity of a vacuum, ε is the dielectric constant of the medium surrounding the particle (80 for an aqueous solution), R is the ideal gas constant, T is the absolute temperature and I is the ionic strength of the solution. c_i and z_i are the concentrations and valences of each type ion in solution, respectively. Making use of Gauss's law together with Eq. 1 it can be shown that the surface potential, ψ_0, is given by:

$$\psi_0 = \frac{\sigma l_D}{\varepsilon_0 \varepsilon} \tag{4}$$

σ is here the surface charge density of the particle. Substituting for ψ_0 from Eq. 4 into Eq. 1 then yields:

$$\psi = \frac{\sigma l_D}{\varepsilon_0 \varepsilon} exp(-r/l_D) \tag{5}$$

The zeta potential, ψ_z, is not exactly the same as ψ_0, because in all measurements of ψ_z, the colloidal-sized particles being investigated act as hydrodynamic objects, meaning that they carry an immobilized layer of solvent with them through solution. ψ_z is then measured at the position of the slip plane, where the solvent is no longer immobilized, not directly at the surface. For lipid membranes in an aqueous solution, the thickness of the immobilized layer has been calculated to be 0.17 (± 0.06) nm [58]. Therefore, substituting $\psi = \psi_z$ and $r = 0.17 \times 10^{-9}$ m into Eq. 7 and rearranging, yields the following equation allowing σ to be calculated from the measured zeta potential and the known ionic strength:

$$\sigma = \frac{\varepsilon_0 \varepsilon}{l_D}\psi_z exp\left(0.17 \times 10^{-9}/l_D\right) \tag{6}$$

Results of the zeta potential obtained at different ionic strengths and the corresponding surface charge densities calculated based on Eq. 6 are given in Table 1. The weighted average of the surface charge density of the membranes across all ionic strengths, weighted according to the reciprocal of the variances of each individual surface charge density, is 0.019 (± 0.001) C m^{-2}. This value is in good agreement with the surface charge density value of 0.023 (± 0.009) C m^{-2} [19], which was found previously to be responsible for the electrostatic interaction stabilising the E2 conformation of the Na^+,K^+-ATPase. Therefore, the results support the conclusion that the interaction which stabilises E2 could be between the N-terminus and the surrounding lipid membrane.

4. Discussion

In an earlier publication [19] we presented evidence that the long-established effects of buffer compounds on the E1/E2 conformational equilibrium could be explained by the degree of buffer ionisation and the consequent influence of the ionic strength in screening an electrostatic attraction which would otherwise stabilise the protein in its E2 conformation. Fitting of the accumulated experimental data obtained from three different buffer compounds (tris, imidazole and histidine) to a series of equations derived from the Gouy-Chapman-theory of the electrical double layer [56,57], enabled us to calculate that the stabilization of the E2 conformation was consistent with an electrostatic attraction to a surface with a charge density of 0.023 (± 0.009) Cm^{-2}. Two possibilities exist for the identity of this surface. One is the protein, i.e., an internal protein-protein interaction, such as a salt bridge, is responsible for the interaction. The other possibility is a protein-membrane interaction, i.e., the protein could be interacting with charges on the surrounding membrane. Here we have considered both these possibilities.

Because mutagenesis studies by the Blostein group [35–37] had previously indicated that a salt bridge might exist between Lys32 and Glu233 within the α_1-subunit of rat Na^+,K^+-ATPase, we first investigated whether this is a possibility based on what is now known about the protein structure. Enhanced sampling REST2 MD simulations utilizing X-ray crystallographic data together with a predicted N-terminus structure indicated that no direct interaction between the corresponding pig sequence residues Lys30 and Glu231 is possible. They are simply spatially too distant to form a salt bridge under normal conditions in either the E1P or E2 states. Thus, although the Blostein group's results indicate that deletion of the residues up to Lys32 and mutation of Glu233 affects the protein's conformation, the conclusion that the observed conformational shifts are due to a disruption of a Lys32-Glu233 salt bridge are unjustified.

Now we turn our attention to the membrane as the possible source of the charged surface with which the protein is interacting. For a lipid bilayer composed of dioleoyl-phosphatidylcholine (DOPC) bilayer, one of the major lipid components of Na^+,K^+-ATPase-containing membrane

Table 1
Zeta potentials, ψ_z, and surface charge densities, σ, of Na^+,K^+-ATPase-containing membrane fragments.*

Ionic strength/mM	ψ_z/mV	σ/C m^{-2} *
10	−61 (± 8)	0.015 (± 0.002)
20	−57 (± 4)	0.020 (± 0.001)
30	−55 (± 6)	0.024 (± 0.003)
40	−40 (± 7)	0.021 (± 0.004)
50	−24 (± 10)	0.014 (± 0.006)
100	−22 (± 8)	0.019 (± 0.007)
150	−17 (± 11)	0.019 (± 0.013)

* The values of σ were calculated from ψ_z and the corresponding ionic strength via Eqs. 4, 5 and 8.

fragments, the cross-sectional area per lipid molecule in the membrane surface is expected to be 0.83 nm^2 or 0.83 × 10^{-18} m^2 [59]. The packing density is the reciprocal of this, thus 1.20 × 10^{18} molecules m^{-2}. If every lipid molecule had a charge of −1, then the charge density would be given by e_0 x 1.20 × 10^{18} molecules m^{-2}, where e_0 is the charge on an electron (1.6 × 10^{-19}C). This would come to 0.193C m^{-2}. However, it's known from lipid analysis [46] that only about 18.6 mol% of the total phospholipids are anionic (i.e., phosphatidylserine (PS) and phosphatidylinositol (PI) or 11.2 mol% of the total lipid (assuming 40 mol% cholesterol). In a cell, virtually all the PS would be on the cytoplasmic side because its asymmetric distribution across the plasma membrane is maintained by flippases. But in the membrane fragments, we can assume that the flippases are no longer active because they require ATP and hence the PS distribution across the membrane would be expected to equalize. Therefore, taking 11.2 % of 0.193C m^{-2}, gives 0.022C m^{-2}. However, this value would be for a pure lipid membrane. The membrane fragments contain a large amount of protein, whose contribution to the surface charge density also needs to be taken into consideration. At neutral pH one would expect all the Asp and Glu residues of the protein to be negatively charged and all the Lys and Arg residues to be positively charged. It is likely, therefore, that these charges would cancel out and the surface charge coming from the protein could be negligible. In the case of the lipids, however, there are no positively charged lipids, only negatively charged ones. So, we can assume that almost all the surface charge comes from the lipid. Nevertheless, the surface area occupied by the protein needs to be considered, because this reduces the net charge density from the lipid.

According to Deguchi et al. [60], who studied the kidney membrane preparation via electronmicroscopy, the protein particles in the membrane have a diameter of 30–50 Å, so let's take 40 Å as the midpoint. The packing density of the protein particles in the membrane they found to be 12,500 μm^{-2}. Based on these values, then, the surface area occupied by a protein molecule in the membrane would be $\pi (d/2)^2 = 3.14$ x $(40 \times 10^{-10}/2)^2 = 1.26 \times 10^{-17}$ m^2. Now, based on the packing density of 12,500 μm^{-2}, the number of protein particles per m^2 would be 12,500 × 10^{12} m^{-2}, and the area in the membrane occupied by these particles would be 12,500 × 10^{12} × 1.26 × 10^{-17} $m^2 = 0.157$ m^2. The percentage of surface area occupied by the protein would be (0.157/1) x 100 = 15.7 %, and hence if all the rest of the membrane is occupied by lipid, the percentage covered by lipid would be 100–15.7 = 84.3 %. Taking this percentage of the charge density value of 0.022C m^{-2} for a pure lipid membrane gives a final value of 0.018C m^{-2}. This is in good agreement with the surface charge density calculated experimentally of 0.023 (± 0.009) C m^{-2} [19] for the surface responsible for stabilising the E2 conformation of the protein.

To test the idea further that the membrane surface is the origin of the charges stabilising E2, we carried out experimental measurements of the zeta potential of the Na^+,K^+-ATPase-containing membrane fragments. Considering the ionic strength of the solution and extrapolating to the surface of the membrane yielded a surface charge density of 0.019 (± 0.003) C m^{-2}, which is consistent with both the calculation just performed and the previously determined value of 0.023 (± 0.009) C m^{-2} [19]. Therefore, all the evidence points to the membrane surface as the origin of the negatively charged surface with which the protein interacts when the E2 conformation is stabilized.

In support of the membrane as an interaction partner for the N-terminus, our REST2 MD simulations demonstrated strong salt bridge interactions between the N-terminal basic side chains and the anionic PS lipid head groups. In the E2 state, this was seen to occur on and off throughout the simulation, while in the E1P state the interaction was maintained indefinitely, despite the dynamics of the protein. Clearly this suggests an important role for the membrane in the mechanism of the Na^+,K^+-ATPase, with the dynamic balance of lipid-protein interactions likely positioning the E2 state to allow regulation, e.g. via phosphorylation by protein kinases [19,61–65]. In fact the N-terminus of the Na^+,K^+-ATPase contains conserved serine and tyrosine residues, which are targets for phosphorylation by protein kinase C and kinases of the Src kinase family, respectively. Phosphorylation of these residues would insert negative charge onto the N-terminus, thus reducing its overall positive charge and weakening its membrane interaction. This is an ideal situation for regulation of the Na^+,K^+-ATPase via an "electrostatic switch" mechanism.

The significant involvement of lipid interactions in the E2 state, but being less than seen in the E1P state, is likely due to the conformational change of the cytoplasmic N and A domains observed between E1P and E2 states. In their recent paper in which they determined several structures of the Na^+,K^+-ATPase in different E1 and E2 conformational states, Guo et al. [27] refer to the first transmembrane helix M1, to which the N-terminus is directly linked, as a "sliding door", which is pulled up by movement of the N and A domains after phosphorylation to close the enzyme's cytoplasmic gate. This movement is likely to be responsible for changes in the degree of interaction of the N-terminus with the surrounding membrane as the enzyme proceeds around its ion pumping cycle.

Now that more structures of the Na^+,K^+-ATPase are available in different conformational states, particularly E1-type states, in the future we would like to repeat the MD simulations presented here using as many different conformational states as possible and using a more physiological membrane composition (noting that the high PS content of the membrane used in the simulations presented here would be expected to overestimate the strength of membrane interaction). In this way it would be possible to visualize movement of the N-terminus on and off the membrane during the ion pumping cycle and to deduce in more detail its involvement in cytoplasmic ion gating and pump regulation.

Finally, it is interesting to note that membrane interaction of the Na^+,K^+-ATPase α_1-subunit N-terminus not only explains the dependence of the enzyme's conformational distribution on ionic strength; it also provides a framework for re-intrepeting the poorly understood effects of Hofmeister anions, such as perchlorate, thiocyanate, iodide and nitrate, on Na^+,K^+-ATPase kinetics. It was first found by Post and Suzuki [66,67] that these anions favour the E1P state over E2P. Later it was shown [68,69] that the effects of the anions on Na^+,K^+-ATPase partial reaction kinetics correlated with their membrane binding ability, suggesting a membrane-mediated effect as the origin of the anion-induced shift in conformational stability. In the light of current knowledge, a possible explanation for the Hofmeister effects on Na^+,K^+-ATPase kinetics could be that by binding to the surrounding membrane, the anions increase the negative surface charge density of the membrane, thereby promoting interaction of the positively charged lysine residues of the N-terminus with the membrane and thus stabilising Na^+,K^+-ATPase conformational states where an N-terminal-membrane interaction is present.

Supplementary data to this article can be found online at https://doi.org/10.1016/j.bbamcr.2023.119539.

Declaration of competing interest

The authors declare that they have no known competing financial interests or personal relationships that could have appeared to influence the work reported in this paper.

Data availability

Data will be made available on request.

Acknowledgement

The authors thank Dr. Thi Hanh Nguyen Pham for providing training in the use of the Nano-ZS Zetasizer. R.J.C. acknowledges financial support from the Australian Research Council (Discovery Grants DP150101112 and DP170101732).

References

[1] J.H. Kaplan, Biochemistry of Na,K-ATPase, Annu. Rev. Biochem. 71 (2002) 511–535.

[2] G. Sachs, J. M. Shin, O. Vagin, N. Lambrecht, I. Yakubov, K. Munson, The gastric H, K ATPase as a drug target: Past, present and future, J. Clin. Gastroenterol. 41 (2007) S226-S242.

[3] D. Diaz, R. J. Clarke, Evolutionary analysis of the lysine-rich N-terminal cytoplasmic domains of the gastric H^+,K^+-ATPase and the Na^+,K^+-ATPase, J. Membr. Biol. 251 (2018) 653–666.

[4] J.P. Morth, B.P. Pedersen, M.S. Toustrup-Jensen, T.L.-M. Sørensen, J. Petersen, J. P. Andersen, B. Vilsen, P. Nissen, Crystal structure of the sodium-potassium pump, Nature 450 (2007) 1043–1049.

[5] T. Shinoda, H. Ogawa, F. Cornelius, C. Toyoshima, Crystal structure of the sodium-potassium pump at 2.4 Å resolution, Nature 459 (2009) 446–450.

[6] R. Kanai, H. Ogawa, B. Vilsen, F. Cornelius, C. Toyoshima, Crystal structure of a Na^+-bound Na^+,K^+-ATPase preceding the E1P state, Nature 502 (2013) 201–206.

[7] M. Nyblom, H. Poulsen, P. Gourdon, L. Reinhard, M. Andersson, E. Lindahl, N. Fedosova, P. Nissen, Crystal structure of Na^+,K^+-ATPase in the Na^+-bound state, Science 342 (2013) 123–127.

[8] K. Abe, K. Irie, H. Nakanishi, H. Suzuki, Y. Fujiyoshi, Crystal structures of the gastric proton pump, Nature 556 (2018) 214–218.

[9] A. Wlodawer, W. Minor, Z. Dauter, M. Jaskolski, Protein crystallography for aspiring crystallographers or how to avoid pitfalls and traps in macromolecular structure determination, FEBS J. 280 (2013) 5705–5736.

[10] T. Ohta, S. Noguchi, M. Nakanishi, Y. Mutoh, H. Hirata, Y. Kagawa, M. Kawamura, The 'lysine cluster' in the N-terminal region of Na^+/K^+-ATPase α-subunit is not involved in ATPase activity, Biochim. Biophys. Acta 1059 (1991) 157–164.

[11] S. Mohammadi, L. Yang, A. Harpak, S. Herrera-Álvarez, M. del Pilar Rodríguez-Ordoñez, J. Peng, K. Zhang, J. F. Storz, S. Dobler, A. J. Crawford, P. Andolfatto, Concerted evolution reveals co-adapted amino acid substitutions in Na^+,K^+-ATPase of frogs that prey on toxic toads, Curr. Biol. 3 (2021) 2530–2538.

[12] S. Asano, K. Miwa, H. Yashiro, Y. Tabuchi, N. Tageguchi, Significance of lysine/glycine cluster structure in gastric H^+,K^+-ATPase, Japan. J. Physiol. 50 (2000) 419–428.

[13] S. E. Faraj, W. M. Valsecchi, N. T. Cerf, N. U. Fedosova, R. C. Rossi, M. R. Montes, The interaction of Na^+, K^+ and phosphate with the gastric H,K-ATPase. Kinetics of E1-E2 conformational changes assessed by eosin fluorescence measurements, Biochim. Biophys. Acta Biomembr. 1863 (2021) 183477.

[14] K.R. Hossain, X. Li, T. Zhang, S. Paula, F. Cornelius, R.J. Clarke, Polarity of the ATP binding site of the Na^+,K^+-ATPase, gastric H^+,K^+-ATPase and sarcoplasmic reticulum Ca^{2+}-ATPase, Biochim. Biophys. Acta Biomembr. 1862 (2020), 183138.

[15] P.L. Jørgensen, J.H. Collins, Tryptic and chymotryptic sites in sequence of α-subunit of (Na^+ + K^+)-ATPase from outer medulla of mammalian kidney, Biochim. Biophys. Acta 860 (1986) 570–576.

[16] P. L. Jørgensen, E Skriver, H. Hebert, A. B. Maunsbach, Structure of the Na,K pump: crystallization of pure membrane-bound Na,K-ATPase and identification of functional domains of the α-subunit. Ann. N. Y. Acad. Sci. 402 (1982) 207–225.

[17] P. L. Jørgensen, J. P. Andersen, Structural basis for E1-E2 conformational transitions in Na,K-pump and Ca-pump proteins, J. Membr. Biol. 103 (1988) 95–120.

[18] P. L. Jørgensen, Purification and characterization of (Na^+,K^+)-ATPase. V. Conformational changes in the enzyme transitions between the Na-form and the K-form studied with tryptic digestion as a tool. Biochim. Biophys. Acta 401 (1975) 399–415.

[19] Q. Jiang, A. Garcia, M. Han, F. Cornelius, H.-J. Apell, H. Khandelia, R. J. Clarke, Electrostatic stabilization plays a central role in autoinhibitory regulation of the Na^+,K^+-ATPase, Biophys. J. 112 (2017) 288–299.

[20] W. Wierzbicki, R. Blostein, The amino-terminal segment of the catalytic subunit of kidney Na,K-ATPase regulates the potassium deocclusion pathway of the reaction cycle, Proc. Natl. Acad. Sci. U. S. A. 90 (1993) 70–74.

[21] S. E. Daly, L. K. Lane, R. Blostein, Functional consequences of amino-terminal diversity of the catalytic subnunit of the Na,K-ATPase, J. Biol. Chem. 269 (1994) 23944–23948.

[22] S. E. Daly, L. K. Lane, R. Blostein, Structure/function analysis of the amino-terminal region of the α1 and α2 subunits of Na,K-ATPase, J. Biol. Chem. 271 (1996) 23683–23689.

[23] F. Cornelius, Y. A. Mahmmoud, L. Meischke, G. Cramb, Functional significance of the shark Na,K-ATPase N-terminal domain. Is the structurally variable N-terminus involved in tissue-specfiic regulation by FXYD proteins? Biochemistry 44 (2005) 13051–13062.

[24] C.H. Wu, L.A. Vasilets, K. Takeda, M. Kawamura, W. Schwarz, Functional role of the N-terminus of Na^+,K^+-ATPase α-subunit as an inactivation gate of palytoxin-induced pump channel, Biochim. Biophys. Acta 1609 (2003) 55–62.

[25] P. Burgener-Kairuz, J.-D. Horisberger, K. Geering, B. C. Rossier, Functional expression of N-terminal truncated α-subunits of Na,K-ATPase in *Xenopus laevis* oocytes, FEBS Lett. 290 (1991) 83–86.

[26] P.T. Nguyen, C. Deisl, M. Fine, T.S. Tippetts, E. Uchikawa, X.-C. Bai, B. Levine, Structural basis for gating mechanism of the human sodium-potassium pump, Nat. Commun. 13 (2022) 5293.

[27] Y. Guo, Y. Zhang, R. Yan, B. Huang, F. Ye, L. Wu, X. Chi, Y. Shi, Q. Zhou, Cryo-EM structures of recombinant human sodium-potassium pump determined in three different states, Nat. Commun. 13 (2022) 3957.

[28] N. Shanbaky, T. A. Pressley, Mammalian α1-subunit of Na^+,K^+-ATPase does not need its amino terminus to maintain cell viability, Am. J. Physiol – Cell Physiol. 267 (1994) C590-C597.

[29] P.L. Else, The highly unnatural fatty acid profile of cells in culture, Prog. Lipid Research 77 (2020), 101017.

[30] T. Utsugi, A.J. Schroit, J. Connor, C.D. Bucana, I.J. Fidler, Elevated expression of phosphatidylserine in the outer membrane leaflet of human tumor cells and recognition by activated human blood monocytes, Cancer Res. 51 (1991) 3062–3066.

[31] S. Ran, J. He, X. Huang, M. Soares, D. Scothorn, P.E. Thorpe, Antitumor effects of a monoclonal antibody that binds anionic phospholipids on the surface of tumor blood vessels in mice, Clin. Cancer Res. 11 (2005) 1551–1562.

[32] S. Riedl, B. Rinner, M. Asslaber, H. Schaider, S. Walzer, A. Novak, K. Lohmer, D. Zweytick, In search of a novel target – phosphatidylserine exposed by non-apoptotic tumor cells and metastases of malignancies with poor treatment efficacy, Biochim. Biophys. Acta Biomembr. 1808 (2011) 2638–2645.

[33] R.J. Clarke, K.R. Hossain, K. Cao, Physiological roles of transverse lipid asymmetry of animal membranes, Biochim. Biophys. Acta Biomembr. 1862 (2020), 183382.

[34] A. Garcia, P.R. Pratap, C. Lüpfert, F. Cornelius, D. Jacquemin, B. Lev, T.W. Allen, R. J. Clarke, The voltage-sensitive dye RH421 detects a Na^+,K^+-ATPase conformational change at the membrane surface, Biochim. Biophys. Acta Biomembr. 1859 (2017) 813–823.

[35] K. Nguyen, A. Garcia, M.-A. Sani, D. Diaz, V. Dubey, D. Clayton, G. Dal Poggetto, F. Cornelius, R. J. Payne, F. Separovic, H. Khandelia, R. J. Clarke, Interaction of N-terminal peptide fragments of the Na^+,K^+-ATPase with membranes, Biochim. Biophys. Acta Biomembr. 1860 (2018) 1282–1291.

[36] K.R. Hossain, D. Clayton, S.C. Goodchild, A. Rodger, R.J. Payne, F. Cornelius, R. J. Clarke, Order-disorder transitions of cytoplasmic N-termini in the mechanisms of P-type ATPases, Faraday Discuss. 232 (2021) 172.

[37] N. Boxenbaum, S. E. Daly, Z. Z. Javaid, L. K. Lane, R. Blostein, Changes in steady-state conformational equilibrium resulting from cytoplasmic mutations of the Na, K-ATPase α-subunit, J. Biol. Chem. 273 (1998) 23086–23092.

[38] L. Segall, L. K. Lane, R. Blostein, New insights into the role of the N terminus in conformational transitions of the Na,K-ATPase, J. Biol. Chem. 277 (2002) 35202–35209.

[39] L. Segall, Z. Z. Javaid, S. L. Carl, L. K. Lane, R. Blostein, Structural basis for α1versus α2 isoform-distinct behavior of the Na,K-ATPase, J. Biol. Chem. 278 (2003) 9027–9034.

[40] I. Klodos, M. Esmann, R.L. Post, Large-scale preparation of sodium-potassium ATPase from kidney outer medulla, Kidney Int. 62 (2002) 2097–2100.

[41] P. Ottolenghi, The reversible delipidation of a solubilized sodium-plus-potassium ion-dependent adenosine triphosphatase from the salt gland of the spiny dogfish, Biochem. J. 151 (1975) 61–66.

[42] G. L. Peterson, A simplification of the protein assay method of Lowry et al. Which is more generally applicable, Anal. Biochem. 83 (1977) 346–356.

[43] O.H. Lowry, N.J. Rosebrough, A.L. Farr, R.J. Randall, Protein measurement with the Folin phenol reagent, J. Biol. Chem. 193 (1951) 265–275.

[44] S. Karmakar, Particle size distribution and zeta potential based on dynamic light scattering: Techniques to characterize stability and surface charge distribution of charged colloids, in U. K. Sur (ed.) Recent Advances in Materials: Physics and Chemistry, Studium Press, New Delhi, India, 2019, pp. 117–159.

[45] S. Jo, T. Kim, V.G. Iyer, W. Im, CHARMM-GUI: a web-based graphical user interface for CHARMM, J. Comput. Chem. 29 (2008) 1859–1865.

[46] J.J.H.H.M. de Pont, A. van Prooijen-Van Eeden, S.L. Bonting, Role of negatively charged phospholipids in highly purified (Na^+ + K^+)-ATPase from rabbit kidney outer medulla studies on (Na^+ + K^+)-activated ATPase, XXXIX, Biochim. Biophys. Acta 508 (1978) 464–477.

[47] W.H.M. Peters, A.M.M. Fleuren-Jakobs, J.J.H.H.M. de Pont, S.L. Bonting, Studies on (Na^+ + K^+)-activated ATPase. XLIX. Content and role of cholesterol and other neutral lipids in highly purified rabbit kidney enzyme preparation, Biochim. Biophys. Acta 649 (1981) 541–549.

[48] J.C. Phillips, R. Braun, W. Wang, J. Gumbart, E. Tajkhorshid, E. Villa, C. Chipot, R. D. Skeel, L. Kale, K. Schulten, Scalable molecular dynamics with NAMD, J. Comput. Chem. 26 (2005) 1781–1802.

[49] A.D. Mackerell Jr., M. Feig, C.L. Brooks 3rd, Extending the treatment of backbone energetics in protein force fields: limitations of gas-phase quantum mechanics in reproducing protein conformational distributions in molecular dynamics simulations, J. Comput. Chem. 25 (2004) 1400–1415.

[50] J.B. Klauda, R.M. Venable, J.A. Freites, J.W. O'Connor, D.J. Tobias, C. Mondragon-Ramirez, I. Vorobyov, A.D. MacKerell Jr., R.W. Pastor, Update of the CHARMM all-atom additive force field for lipids: validation on six lipid types, J. Phys. Chem. B 114 (2010) 7830–7843.

[51] S.E. Feller, Y. Zhang, R.W. Pastor, B.R. Brooks, Constant pressure molecular dynamics simulation: the Langevin piston method, J. Chem. Phys. 103 (1995) 4613–4621.

[52] J.P. Ryckaert, G. Ciccotti, H.J.C. Berendsen, Numerical-integration of Cartesian equations of motion of a system with constraints – molecular dynamics of n-alkanes, J. Comput. Phys. 23 (1977) 327–341.

[53] U. Essmann, L. Perera, M.L. Berkowitz, A smooth particle Ewald method, J. Chem. Phys. 103 (1995) 8577–8593.

[54] L.L. Wang, R.A. Friesner, B.J. Berne, Replica exchange with solute scaling: a more efficient version of replica exchange with solute tempering (REST2), J. Phys. Chem. B 115 (2011) 9431–9438.

[55] I. Nahringbauer, Hydrogen bond studies. XX. The crystal structure of ammonium formate, Acta Cryst. B24 (1968) 565–570.

[56] P.C. Hiemenz, Principles of Colloid and Surface Chemistry, 2nd ed., Marcel Dekker, New York, 1986, pp. 686–703.

[57] G. Adam, P. Läuger, G. Stark, Physikalische Chemie und Biophysik, 2nd ed., Springer, Berlin, Germany, 1988, pp. 276–277.

[58] V. Knecht, B. Klasczyk, R. Dimova, Macro- versus microscopic view on the electrokinetics of a water-membrane interface, Langmuir 29 (2013) 7939–7948.
[59] R.J. Clarke, Effect of lipid structure on the dipole potential of phosphatidylcholine bilayers, Biochim. Biophys. Acta Biomembr. 1327 (1997) 269–278.
[60] N. Deguchi, P.L. Jørgensen, A.B. Maunsbach, Ultrastructure of the sodium pump: comparison of thin sectioning, negative staining, and freeze facture of purified membrane-bound (Na^+, K^+)-ATPase, J. Cell Biol. 75 (1977) 619–634.
[61] E.-L. Blayney, M. Chennath, C.G. Cranfield, R.J. Clarke, Bioinformatic analysis of Na^+,K^+-ATPase regulation through phosphorylation of the alpha-subunit N-terminus, Int. J. Mol. Sci. 24 (2023) 67.
[62] Y.A. Mahmmoud, F. Cornelius, Protein kinase C phosphorylation of purified Na,K-ATPase: C-terminal phosphorylation sites as the α- and γ-subunits close to the inner face of the plasma membrane, Biophys. J. 82 (2002) 1907–1919.
[63] A.V. Chibalin, C.H. Pedemonte, A.I. Katz, E. Feraille, P.O. Bergren, A.M. Bertorello, Phosphorylation of the catalytic α-subunit constitutes a triggering signal for Na^+,K^+-ATPase endocytosis, J. Biol. Chem. 273 (1998) 8814–8819.
[64] A.V. Chibalin, G. Ogimoto, C.H. Pedemonte, T.A. Pressley, A.I. Katz, E. Feraille, P. O. Bergren, A.M. Bertorello, Dopamine-induced endocytosis of Na^+,K^+-ATPase is initiated by phosphorylation of Ser-18 in the rat α subunit and is responsible for decreased activity in epithelial cells, J. Biol. Chem. 274 (1999) 1920–1927.
[65] M.S. Feschenko, K.J. Sweadner, Structural basis for species-specific differences in the phosphorylation of Na,K-ATPase by protein kinase C, J. Biol. Chem. 270 (1995) 14072–14077.
[66] R.L. Post, K. Suzuki, A Hofmeister effect on the phosphoenzyme of Na,K-ATPase, in: J.H. Kaplan, P. De Weer (Eds.), The Sodium Pump: Structure, Rockefeller University Press, New York, USA, Mechanism and Regulation, 1991, pp. 201–209.
[67] K. Suzuki, R.L. Post, Equilibrium of phosphointermediates of sodium and potassium ion transport adenosine triphosphatase. Action of sodium ion and Hofmeister effect, J. Gen. Physiol. 109 (1997) 537–554.
[68] R.J. Clarke, C. Lüpfert, Influence of anions and cations on the dipole potential of phosphatidylcholine vesicles: a basis for the Hofmeister effect, Biophys. J. 76 (1999) 2614–2624.
[69] C. Ganea, A. Babes, C. Lüpfert, E. Grell, K. Fendler, R.J. Clarke, Hofmeister effects of anions on the kinetics of partial reactions of the Na^+,K^+-ATPase, Biophys. J. 77 (1999) 267–281.